Yield, impact and fracture performance of injected metallic looking polypropylene parts

A. Costantino, P. Frontini, V. Pettarin
Polymer Science & Engineering Group, Institute of Materials Science and Technology, University of Mar del Plata – CONICET, Mar del Plata, Argentina

A. Pontes
Institute for Polymer and Composites/I3N, University of Minho, Guimarães, Portugal

ABSTRACT: Innovation, cost and weight reduction are some factors for the replacement of metals by plastics. Plastics continue to offer attractive solutions for design engineers. The metallic effect obtained by incorporation of metal particles in polymers by injection moulding has the advantage of eliminating post-processing techniques reducing production cost and time. Nevertheless, undesired defects in the final appearance of parts are common. These defects occur due to inhomogeneous orientation and anisotropy of the metal particles. Very few studies are reporting the influence of metallic particles on the morphology development of PP parts. Therefore, this study is focused on the production of parts made of PP/metallic pigments (aluminium) by injection moulding in order to understand the influence of metallic particles on the aesthetic, morphological and mechanical properties of the parts.

1 INTRODUCTION

Nowadays, the use of composite materials in different fields of engineering (microelectronics, aeronautics and space, transport, etc.) is continually increasing (Xu et al. 2001; Thongruang et al. 2002; Korab et al. 2002; Chen et al. 2002; Yu et al. 2002). The interest for these materials arises from the fact that it is possible to develop new materials with properties adapted to specific applications. Moreover, in some cases, composite materials allow the physical properties of each component used in the manufacturing process to be combined. In recent years, new materials and new technologies have been developed to eliminate the existing gaps in terms of aesthetic products. The metallic effects of the plastics came to revolutionize the automotive industry, packaging and appliances, replacing the metal by plastic in various components. Thus, attributing the quality and prestige of the metal and adding value to products (Wheeler 1999).

The imitation of metal by plastic has increased notably through the addition of metallic pigments in thermoplastic resins. The composite obtained has the main advantage of eliminating post-processing operations. Metal particles have different sizes and shapes. Those having a plate like shape promote the increase of reflected light in a specular way, increasing the lustre and metallic appearance of surfaces (Bunge 1998).

Nonetheless, the appearance of flow lines and welded lines caused by the orientation of the pigment flakes perpendicularly to the surface (Kobayashi et al. 2011; Harris 1999) significantly affects the appearance of the injection moulded part. These defects can be minimized by adjusting the processing conditions. It has been pointed out that an increase in mould and injection temperatures causes the disorientation of flakes, which in turn, attenuates weld/flow lines. The changing of size and size distribution of metal particles are alternatives to minimize these defects (Park et al. 2012; Kobayashi et al. 2011; Martins et al. 2012; Harris 1999).

In structural and semi-structural applications of materials, in addition to high stiffness and mechanical strength, adequate fracture toughness is often required. In order to optimize these properties, the knowledge of the relationship between morphology and deformation behaviour seems to be essential. It is known that the macroscopical behaviour of heterogeneous polymer based materials depends on many factors such as composition, behaviour of each component, geometrical arrangement of the phases, and interfacial properties (Móczó & Pukánszky

2008; Fu et al. 2008). The behaviour of PP based composites in engineering applications critically depends on the extent of crystallinity and the nature of the crystalline morphology of PP (Greco et al. 2007; Xu et al. 2003).

The influence of processing parameters is critical in the performance of these products. Features like mechanical properties and morphology of injection moulded composites, strongly depend on thermomechanical processing variables (Viana et al. 1997). In the case of injection moulded semi-crystalline polymers, crystal properties are highly influenced by processing conditions. It is noteworthy that by compounding and processing (thermally, mechanically) of different polymers and reinforcements can be explored diversity of morphologies. Change of the structure on molecular or macroscopic level may improve dramatically mechanical properties, e.g. modulus, stiffness and impact strength (Powell & Beall 2006; Viana et al. 2004; Rojek & Stabik 2009; Dobrzanski et al. 2008; Wróbel et al. 2009) as well as toughness and flexural modulus.

The present work aims to evaluate the influence of the addition of aluminium pigment on the performance of PP injected mouldings. A complete characterization is therefore reported, which includes an aesthetical analysis, morphological evaluation and mechanical and fracture characterization. A double gated mould was used, in which a weld line is formed by melt fronts meeting at different angles, and a distribution of molecules and particles orientation is generated from the injection points. The influence of singularities induced by flow pattern such as weld lines and injection points on the arrangement of mechanical performance in the moulding was explored.

2 EXPERIMENTAL

2.1 *Materials and processing*

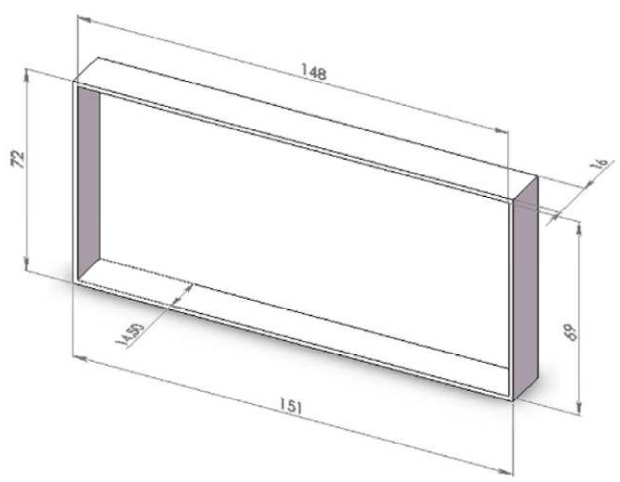

Figure 1. Scheme of mouldings.

Polypropylene (PP) copolymer powder from ICORENE with specific gravity of 0.9 Mg/m^3 and a melt flow index of 13 g/10 min (190 ºC, 2.16 kg), was used in this study. The pigment used was Silberline 21075 aluminium particles of 75 microns provided by Poliversal S.A. which consists of 70 % nominal weight of Al particles and 30 % nominal weight of carrier, and is compatible with a wide range of thermoplastics (Technical sheet). A previous study indicated that Al particles had a flake like shape (Martins et al. 2012). The mixture of metallic particles with PP was done in a rotary drum, using 2 wt% of metal particles; the percentage used was based on a previous work (Martins et al. 2012).

Two gated boxes (Fig. 1) of dimensions: 152 mm width, 73mm length, 16 mm height and 1,5 mm thick were processed in an injection moulding machine Ferromatik-Milacron K85. The processing conditions are listed in Table 1. To determine the influence of processing conditions on morphology and therefore in performance of mouldings, injection temperature (T_{inj}) and mould temperature (T_{mould}) were varied according to Table 2.

Table 1. Injection moulding parameters.

Processing parameters	Value
Injection speed	60 mm/s
Injection pressure	45 bar
Injection time	1 s
Packing pressure	35 bar
Packing speed	30 mms/s
Packing time	5 s
Cooling time	20 s
Cycle time	34 s

Table 2. Variable injection moulding parameters.

Condition	Tinj (ºC)	Tmold (ºC)
1	190	25
2	190	40
3	190	55
4	190	70
5	220	70
6	220	55
7	220	40
8	220	25
9	250	25
10	250	40
11	250	55
12	250	70

2.2 *Aesthetical analysis*

Besides the aesthetic analysis and defects that are seen with the naked eye, the superficial distribution of Al particles in PP mouldings was observed with an optical metallographic microscope Olympus PMG3. Obtained micrographs were analysed with the software ‘Image Pro Plus’ and superficial percentage of Al particles obtained.

2.3 *Morphological analysis*

XRD analysis was performed using a Phillips X'PERT MPD diffractometer in reflection mode (Cu Kα radiation λ = 1.5418 °A, generator voltage 40 kV, current 40 mA, sample to detector distance 240 mm) to observe the PP structure in the skin and the core according to Figure 2. Measurements were recorded every 0.02 ° for 1 s each, varying 2θ from 5 ° to 45 °. The fraction of β-phase in the crystalline phase of polypropylene was calculated by using the Turner Jones relation (Turner Jones et al. 1964):

$$K_\beta = \frac{I^\beta_{300}}{I^\beta_{300} + I^\alpha_{110} + I^\alpha_{040} + I^\alpha_{130}} \quad (1)$$

where in a generic sense I^i_{abc} is the intensity of the (*abc*) crystal growing plane for each phase *i*.

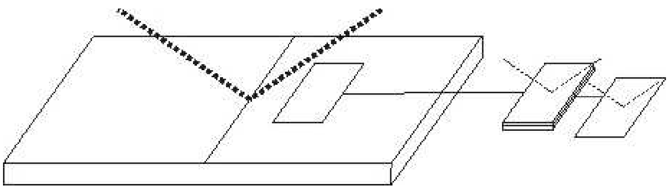

Figure 2. Setup for the XRD observations made on injection moulded boxes.

DSC tests were performed on specimens that included part of the skin and part of the core structure using Perkin-Elmer equipment at a heating rate of 10 °C min^{-1} and at 2 °C min^{-1} to distinguish the fusion of β-PP polymorph ( ) from α-PP ($T_m \approx 165°C$) (Karger-Kocsis 1996). The average global crystallinity was calculated as:

$$x_c = \frac{\Delta H}{(1-\phi)\Delta H^0} \quad (2)$$

where ΔH is the apparent enthalpy of fusion per gram of composite, ΔH^0 is the heat of fusion of 100 % crystalline PP, which is 207.1 kJ kg^{-1}(Brandrup & Immergut 1999) and ϕ is the Al particles weight fraction.

2.4 *Mechanical and fracture analysis*

Tensile tests were performed in an Instron 4467 universal testing machine, at room temperature and at a speed of 1 mm/min. The tensile bars were cut in the same locations described in Figure 3, so reporting the mechanical properties in the welded region of mouldings. Yield stress, σ_y, was assessed as the maximum value of the stress-strain curve.

Fracture characterization was carried out on mode I double edge-notched tensile specimens (DENT) cut from the mouldings (nominal width, *W*, of 30 mm, nominal crack to depth ratio, *a*/*W*, of 0.5, and nominal length, *S*, of 70 mm), at a crosshead speed of 2 mm/min and room temperature in an Instron 4467 universal testing machine. Sharp notches were introduced by scalpel-sliding a razor blade having an on-edge tip radius of 13 µm with a Ceast Notchvis notching machine. In order to assess influence of the weld lines in fracture, DENT samples were cut from different places of the mouldings (with and without weld lines) as depicted in Figure 3.

The initiation fracture toughness was evaluated as the stress intensity factor at 5 % non-linearity (Williams 2001). The load at crack initiation F_q was determined as the intercept between the load curve and the *C* + 5 % compliance line, *C* being the initial compliance of the load–displacement curve. The stress intensity factor at initiation, K_{Iq} was then determined as:

$$K_{Iq} = \frac{F_q}{B\sqrt{\frac{W}{2}}} f\left(\frac{a}{W}\right) \quad (3)$$

where *B* is the thickness of the sample, *W* is the width of the sample, a is the length of the notch, and *f*(*a*/*W*) is the function of the notch to width that for DENT samples is:

$$f\left(\frac{a}{W}\right) = \frac{\sqrt{\frac{\pi a}{2W}}}{\sqrt{1-\frac{a}{W}}}\left[1.122 - 0.561\left(\frac{a}{W}\right) - 0.205\left(\frac{a}{W}\right)^2 + 0.471\left(\frac{a}{W}\right)^3 + 0.19\left(\frac{a}{W}\right)^4\right] \quad (4)$$

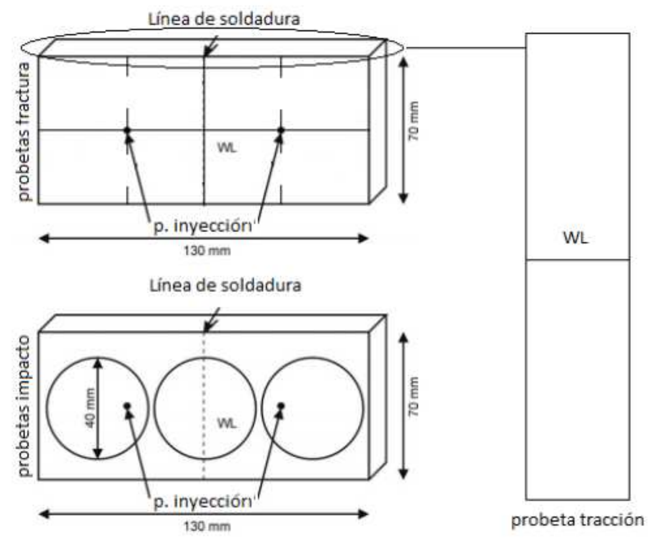

Figure 3. Location of tensile, DENT and disc samples.

Biaxial impact tests were carried out according to ASTM D 3763-93 in two locations of the pieces (on and out of weld line) (Fig. 3) using an instrumented Ceast Fractovis 6787 falling weight equipment. The specimens were clamped between two steel plates with a circular opening of 40 mm in diameter and tested at 3.5 m/s and room temperature. The biaxial impact toughness, *J*, was calculated as the total energy to break the sample (total area over the force-displacement curve) divided thickness. Biaxial impact tests are tests on representative samples, rather than measurements of basic material properties on standard test pieces, which give a realistic view of in service impact situations—being closer to real life conditions—with the additional advantage that they provide a convenient method of studying changes induced by flow in moulded part performance (Cunha et al. 1992; Viana et al. 1997).

2.5 *Fractography*

Fracture surfaces of broken samples were analysed using a JEOL JSM-6460LV scanning electron microscope (SEM) at an accelerating voltage of 20 kV. Samples were sputter coated with a thin layer of gold before they were observed.

3 RESULTS AND DISCUSSION

3.1 *Aesthetical analysis*

Metallic pigments offer exceptional silver effects on the polymeric matrix, as can be observed in Figure 4. However, there are visual defects that are important to analyse because they are directly related to the final quality of the mouldings. It is clearly seen that the incorporation of Al pigment in PP matrix made weld lines and some flow lines evident. These defects have been reported in literature (Rawson 1999). The orientation of the particles and its anisotropic character in terms of reflection of light causes the appearance of a dark line at the surface of the part (Harris 1999).

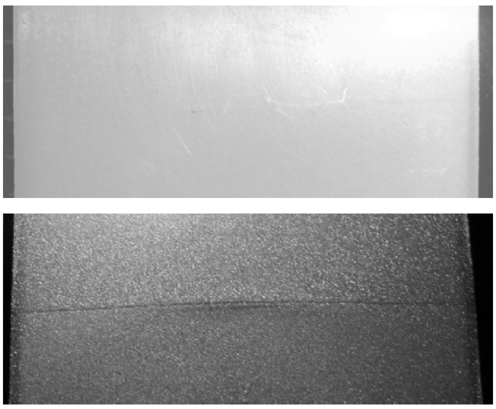

Figure 4. Weld line zone in boxed (a) PP (b) PP/Al.

Regarding processing conditions, aesthetic differences were observed between pieces obtained under varying injection temperatures. Less warpage, less differential shrinkage and less noticeable welding lines were observed at higher T_{mold} and T_{inj} (Fig. 5) in both materials (PP and PP/Al). In PP/Al mouldings, at lower T_{mold} and T_{inj} flow lines near injection point are more visible and distorted given the final part an unsightly appearance.

A good dispersion of Al particles was observed away from flow and weld lines by optical microscopy (Fig. 6). Also a beneficial orientation was observed, i.e. flakes with reflecting surface parallel to part surface. All samples presented a good dispersion and orientation of pigment away from injection points and weld lines. However, in weld lines a lower amount of reflecting particles is observed in the surface (6 % vs 22 % away from weld line). In the weld region the particles flake adopt the orientation imposed by the flow lines. Therefore, when two flow fronts meat each other a weld line is formed. The rapid solidification of the melt due to the contact with the mould does not allow the reorientation of the particles at that location. Thus particles remain perpendicular to the plane of the surface, and a dark line appears (Park et al. 2012; Martins et al. 2012). Weld lines appeared wider and diffuser with increasing melt temperature (Fig. 7). Melt viscosity influences the ability of the polymer to transport the metallic pigment in the melt front during injection moulding. At higher temperature lower melt viscosity and therefore the flux between flake particles is easer (Wheeler 1999). Another feature of weld lines is that the wide changes with distance to the border of the moulding, evolving to two weld lines in the centre. Also, radial flux lines appeared near injection points (Fig. 6).

Condition 1	Condition 12
T_{mold}=25°C	T_{mold}=70°C
T_{inj}=190°C	T_{inj}=250°C

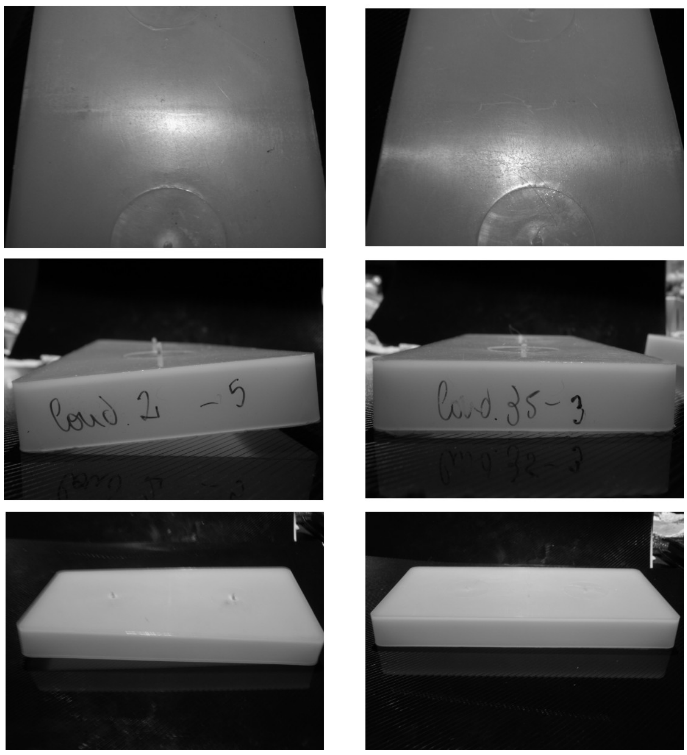

Figure 5. Main defects of injection mouldings of PP/Al.

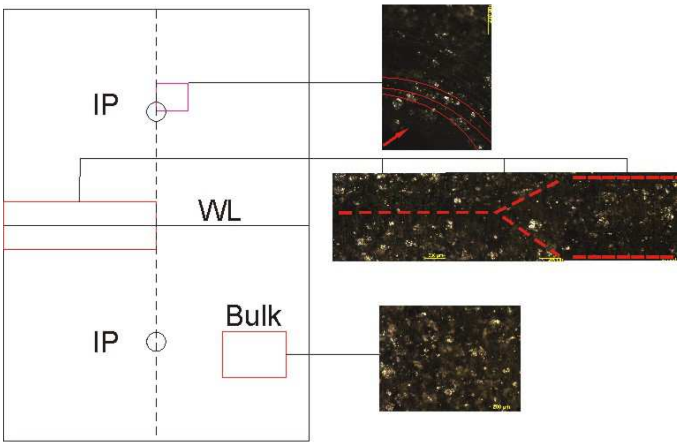

Figure 6. Optical microscopy photos of mouldings.

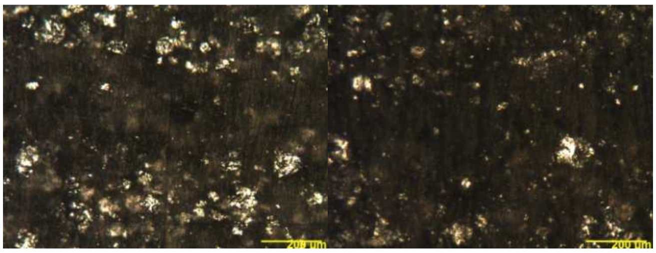

Figure 7. Weld lines zones (a) condition 1 (b) condition 12.

3.2 *Morphological analysis*

XRD showed that the metallic pigment induced noticeable differences in PP morphology of the samples skin (Fig. 8). The addition of the pigment with the carrier promoted the formation of β-PP (increase in (300) reflection, Fig. 8a), decreasing crystallinity (decrease of reflections intensity). Regarding processing conditions, mould temperature greatly influences the microstructure: increasing temperature in 45 °C duplicates the percentage of β-PP in both pure PP and PP/Al mouldings (Fig. 8b). However, melt temperature does not influence the microstructure (Fig. 9).

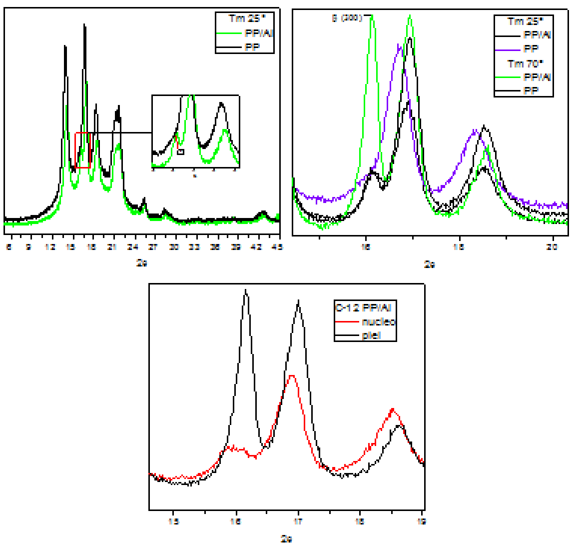

Figure 8. DRX curves of PP and PP/Al mouldings. (a) condition 1 (b) processed at different temperatures (c) comparison between skin and core of PP/Al moulding processed at condition 12.

The β content distribution was determined in samples of processing condition 12. There is a profile of β content trough the samples (Table 3). In weld lines K_β is lower than in the bulk, which is in agreement with previous findings (Wenig et al. 1990). Big differences in K_β were found between skin and core. It was seen that the 300 diffraction maximum of β-phase decreases from the skin to the core (see Fig. 8c). For example, away from weld lines in PP-Al boxes, K_β diminished from 0.34 to 0.16 as moving from the skin to the core. The first attempt to justify this fact is to attribute it to differences in Al particles and carrier concentration between skin and core. However, it was seen by optical microscopy that there is a good distribution of the pigments in the samples but they tend to accumulate in the central region of the core (Fig. 10a). As a consequence, if the carrier particles were acting as nucleating agents, tendency should be the contrary. It seems that the responsible of high content of β-PP in the skin are the carrier particles along with the shear developed during processing. In the microstructure of PP part along the thickness direction it is possible to observe a typical structure of an injection-moulded part consisting of skin, shear layer and core (Fig. 10b). Due to the sudden cooling of the part in the cold mould walls, the skin is characterized by very high chain orientation. The shear layer appears between the skin and the core and is characterized by having an undeveloped spherulitic structure. Finally, in the core, well developed spherulitic structure is observed. PP/Al shows an increased size of skin compared to the PP (Santos et al. 2013). This is due to the higher thermal conductivity of aluminium which provides a faster cooling rate and consequently an increase of the skin thickness. In the shear layer it is observed the formation of transcrystalline structures around the particles. The transcrystalline structures are characterized by having a high density of crystals formed at the surface of the metal particles, inhibiting the normal spherulitic growth (α-PP). As a consequence, β-PP forms preferentially under the shear stresses of the skin and the shear layer.

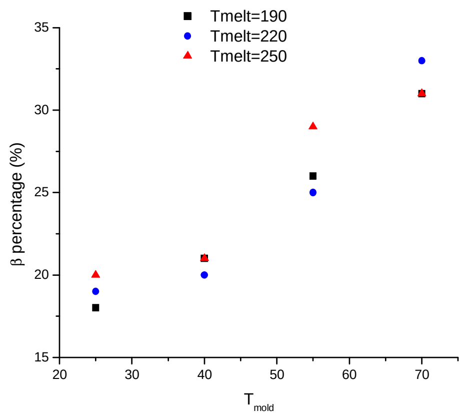

Figure 9. β-PP polymorph as a function of mould temperature.

Table 3. β content (K_β) in skin of samples of processing condition 12.

Sample	K_β in weld line	K_β in bulk
PP	0.11	0.19
PP-Al	0.30	0.34

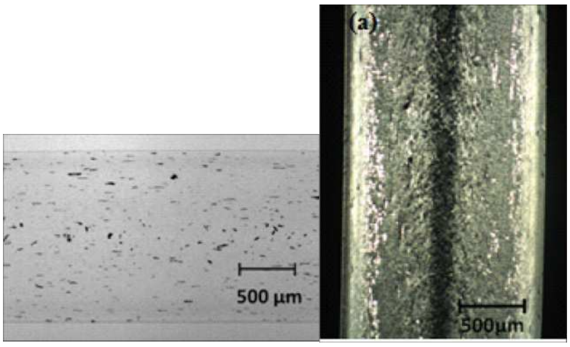

Figure 10. Optical microscopies of PP-Al parts (a) transmitted light (b) polarized light.

DSC analysis indicated that global crystallinity was not affected by variation in processing parameters, and pieces of neat PP have a slightly higher crystallinity (0.34) than pieces of PP-Al (0.30). At 2 °C/min the presence of β-PP was evident (Fig. 11).

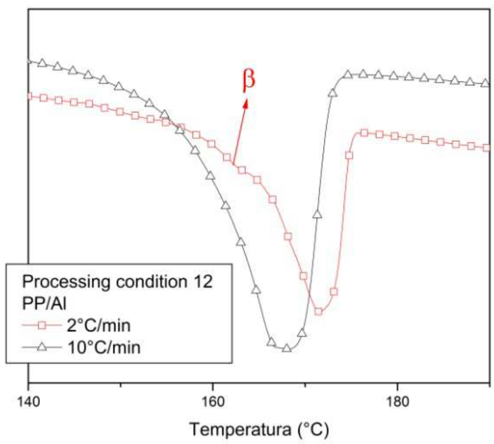

Figure 11. DSC thermograms for typical PP-Al parts.

3.3 *Mechanical analysis*

3.3.1 *Yield behaviour*

Yield stresses – determined at the weld lines – of injected pieces slightly diminished with the addition of Al particles and did not vary significantly for varying injection parameters (Table 4). Tendency agrees with similar materials reported in literature (Martins et al. 2012; Maiti & Mahapatro 1992).

However, the post-yielding performance is distinct for different materials and processing conditions (Fig. 12). PP mouldings behaved in a ductile manner. Stress whitening was observed in the zone subjected to tensile stress, making evident the weld line, which became white and well defined. In the weld line a neck occurred, and finally the sample failed. For PP-Al composites two different behaviours were observed depending on mould temperature. Pieces injected at low mould temperature exhibited craze formation which initiate at the V-notch of the weld line, followed by holes coalescence. Also a “skin-core” effect is observed, with differences in deformation between these zones. PP-Al pieces injected at high mould temperature behaved in a brittle manner failing at the weld line with no plastic deformation. It is interesting to note that all PP-Al pieces presented lower post-yield deformation that PP pieces.

Table 4. Yield stress of mouldings for extreme processing conditions.

σ_y (MPa)	C-1	C-12
PP	19.0	19.5
PP-Al	17.5	18.0

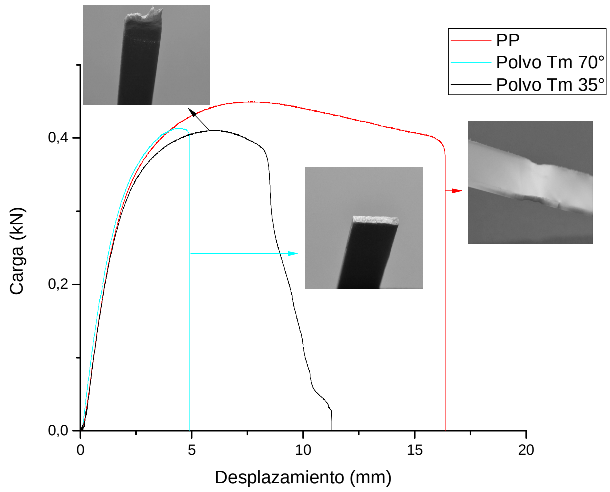

Figure 12. Typical load-displacement curves under tensile stress for samples with weld lines.

This limited plastic deformation capability of injected PP-Al pieces at the weld line can be easily explained by different contributions: (a) initial deformation begins at the weld line when a stress concentrating surface groove is present (Hobbs 1974) and in PP-Al pieces a surface V-notch is present at the weld line that acts as a stress concentration; (b) sample morphology near the knit line can be a determining factor in failure (Hobbs 1974; Wenig 1990), and in these samples differences in global crystallinity, β-PP content and Al particles distribution were observed, which determined large inhomogeinities near the knit line; (c) finally, flake particles generate larger contact stresses and are not capable to transfer load (Osman & Mariatti 2006).

3.3.2 *Fracture behaviour*

Injected pieces of PP and PP-Al presented similar behaviour in fracture tests performed away from weld lines. All samples exhibited non-lineal behaviour with crack stable propagation and large plastic deformation (Fig. 13). Also, initiation and propagation fracture parameters were similar (Table 5). A slight difference was observed for propagation values, PP pieces being a little more ductile than PP-Al mouldings.

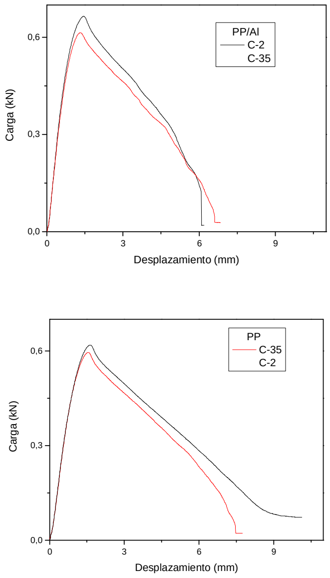

Figure 13. Typical load-displacement curves of fracture tests for samples without weld lines.

Table 5. Fracture parameters for extreme processing conditions.

	K_{Ic} (MPa.m$^{1/2}$)		G_{Ic} (J)	
	C-1	C-12	C-1	C-12
PP	2.0	1.7	87	86
PP-Al	2.0	1.8	75	72

An important difference was observed between plastic shape of PP and PP-Al pieces: plastic zones of PP pieces were diamond shaped while PP-Al pieces developed elliptic plastic zones (Fig. 14). This is due to differences in polymorphic phase: α-PP develops a diamond shaped plastic zone and β-PP develops an elliptic plastic zone (Karger-Kocsis 1996).

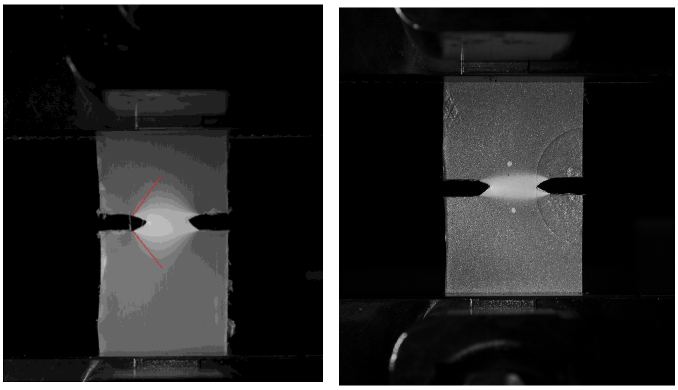

Figure 14. Plastic zones developed in fracture tests for (a) PP (b) PP-Al mouldings.

Also, differences in propagation mode were observed in SEM (Fig. 15). Skin and core behaviour were very different, the core presenting larger plastic deformation. PP-Al injected samples presented more ductile deformation than PP mouldings. This is due to the presence of β-PP, which is more ductile and tough than α-PP (Karger-Kocsis 1996; Chen et al. 2002). Toughness improvement of β-PP was attributed to the development of a more perfect crystalline structure, with higher continuity of the amorphous phase and more connecting bridges between individual crystallites than a material containing solely α-crystallites (Kotek et al. 2002); and to the occurrence of a β-α transformation during loading which is accompanied with volume contraction in respect to the related crystallographic densities (Karger-Kocsis & Varga 1996).

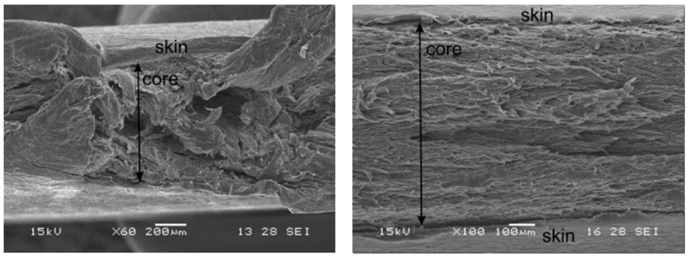

Figure 15. SEM micrographs of fractured samples (a) PP; (b) PP-Al.

Al particles acted as stress concentrators being not bonded to PP (Fig. 16) and therefore diminishing toughness. In summary, the occurrence of □-PP in PP-Al mouldings contrast the detrimental effect of Al flakes, and PP-Al mouldings have similar toughness as PP mouldings.

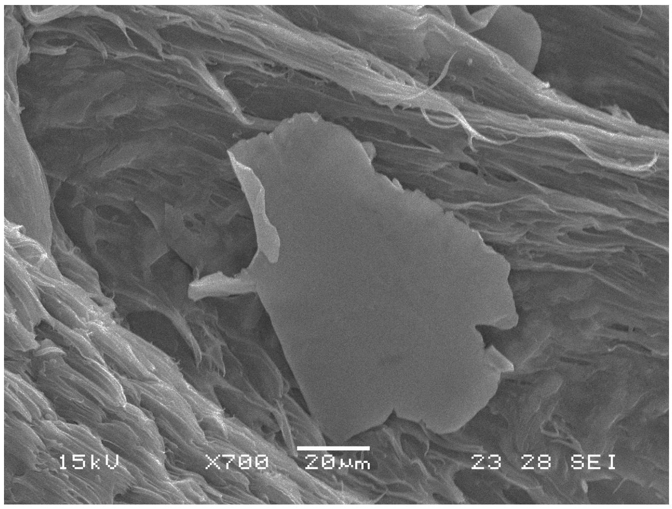

Figure 16. SEM micrographs of PP-Al fractured sample in which a de-bonded Al flake is clearly seen in deformed PP.

3.3.3 *Impact behaviour*

Typical behaviour – at the weld line zone – of PP and PP-Al parts under impact loads are shown in figure 17. PP behaved in a semi ductile manner, with whitening of the impacted zone before fracture (Fig.

17a), while PP-Al exhibited a completely brittle failure (Fig. 17b). It seems that Al particles act as defects with the unfavourable orientation of Al flakes near the weld line prevailing, and the benefits of the β phase are mostly inhibited by high solicitation rates. It is noticeable that all samples (PP and PP-Al) failed following the weld line, i.e. it acts as a strong stress raiser defect.

When samples were impacted near the injection point a similar failure was observed. In figure 18 a comparison between behaviour at the weld line and near injection point is shown. Flux lines act as stress raisers, in the same way as a weld line.

It is interesting to note that PP-Al samples with higher β-PP content exhibited better impact energy than samples with lower β-PP content (Table 6), indicating that the behaviour can be improved changing the morphology by processing conditions.

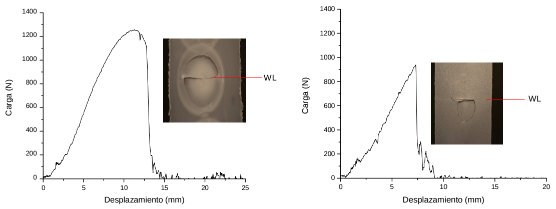

Figure 17. Typical behaviour under biaxial impact at the weld line for (a) PP (b) PP-Al mouldings (processing condition 12).

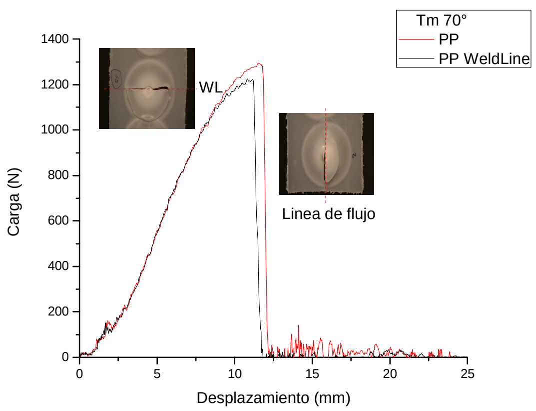

Figure 18. Comparison of behaviour under biaxial impact at the weld line and near injection point (PP samples).

Table 6. Biaxial impact energy for extreme processing conditions.

	At weld line		Near injection point	
	C-1	C-12	C-1	C-12
PP	7.8 J	8.1 J	6.7 J	7.1 J
PP-Al	3.5 J	3.7 J	2.8 J	4.1 J

CONCLUSIONS

The addition of Al particles in PP matrix has influence on the aesthetical, morphological and mechanical properties of injection moulded parts. The metallic looking effect is easily obtained when these particles are used, at low weight percentages (max 2 %). However, several types of undesired effects appear, such as weld lines and warpage that are dependent on the processing conditions used.

In terms of aesthetics effects, higher mold and melt temperatures induced less warpage, less differential shrinkage and less noticeable welding lines, indicating that aesthetic aspects could be improved by manipulating processing conditions. Optical microscopy of the welded zone showed the orientation of the particles with the flow lines, and a lower amount of reflecting particles observed in the surface. There particles remained perpendicular to the plane of the surface, and a dark line appeared. Weld lines appeared wider and diffuser with increasing melt temperature.

Morphology analysis showed a distinction between PP and PP-Al moulded parts. The carrier of the Al particles induced the formation of β-PP phase and slightly diminished global crystallinity. This nucleating effect was found to be dependant of processing conditions: higher melt temperature induced higher β-PP content.

Regarding yielding, yield stress was not affected by the addition of Al particles. However, all PP-Al pieces presented lower post-yield deformation that PP pieces.

Fracture parameters under quasi-static loading conditions were actually the same for PP and PP-Al moulded parts. However, plastic zones of PP pieces were diamond shaped (typical of α-PP) while PP-Al pieces developed elliptic plastic zones (typical of β-PP). Also, differences in propagation mode were observed in SEM. The occurrence of β-PP in PP-Al mouldings balanced out the detrimental effect of Al flakes, and PP-Al mouldings have similar toughness as PP mouldings, under triaxial quasi-static loading conditions.

However, under biaxial impact loading these beneficial effects of β polymorph are inhibited, and the defects induced by Al flakes orientation and their poor adhesion to the PP matrix prevailed.

REFERENCES

Brandrup J. and E. H. 1999. Immergut. Polymer Handbook New York, Wiley.

Bunge, H. 1998. Metallic looking plastics with new silver and colored aluminum pigments. Paper presented at the Annual Technical Conference - ANTEC, Conference Proceedings,3, 2586-2588

Chen H. B., J. Karger-Kocsis , J. S. Wu and J. Varga. 2002. Fracture toughness of α- and β-phase polypropylene homopolymers and random- and block-copolymers. *Polymer* Vol. 43 p. 6505-6514.

Chen, Y. M.; Ting, J. M. Carbon. 2002. 40, 359–362

Cunha A.M., A.S. Pouzada, and R.J. Crawford. 1992. Plast. Rubber Compos. Pro. 18, 79.

Dobrzanski, L.A., Grajcar, A., Borek, W. 2008. Microstructure evolution and phase composition of high-manganese austenitic steels. *Journal of Achievements in Materials and Manufacturing Engineering* 31/2, 218.

Fu S-Y, Feng X-Q, Lauke B, Mai Y-W. Effects of particle size, particle/matrix interface adhesion and particle loading on mechanical properties of particulate–polymer composites. *Composites:* Part B 2008;39:933–61.

Greco A, Musardo A, Maffezzoli A. 2007. Flexural creep behaviour of PP matrix woven composite. *Compos Sci Technol* 67:1148–58.

Harris, R. M. *Coloring Technology for Plastics.* 1999. New York: Plastics Design Librar,. ISSN 1-884207-78-2.

Hobbs S. Y. 1974. Some observations on the morphology and fracture characteristics of knit lines. *Polymer Engineering and Science* Vol. 14(9) p. 621-626.

Karger-Kocsis J, Varga J. 1996. Effects of □-□ transformation on the static and dynamic tensile behaviour of isotactic polypropylene, *J. of Applied Polymer Science* 62: 291-300.

Karger-Kocsis J. 1996. How does Phase Transformation Toughening" Work in Semicrystalline Polymers. *Polymer Engineering and Science,* Vol. 36: 203-210.

Kobayashi, Y. et al. 2011. The unique flow of polypro-pylene at the weld line behind an obstacle in injection molding. *Journal of Polymer Engineering and Science* 51 (3): 526-531.

Korab, J.; Stefanik, P.; Kavecky, S.; Sebo, P. Korb, G. 2002. *Compos A,* 33: 577–581.

Kotek J, Raab M, Baldrian J, Grellmann W. 2002. The effect of specific □-nucleation on morphology and mechanical behaviour of isotactic propylene. *J. of Applied Polymer Science* 85: 1174-1184.

Maiti S. N. and P. K. Mahapatro. 1992. Mechanical properties of nickel-powder-filled polypropylene composites. *Polymer Composites* Vol. 13(1): 47-52.

Martins C.I., I. Santos and A.J. Pontes. 2012. On the effect of metallic particles on the performance of injection moulded PP plastic parts. Conference on Polymer and Mold Innovations, p. 375-382.

Móczó J, Pukánszky B. 2008. Polymer micro and nanocomposites: structure, interactions, properties. *J Ind Eng Chem* 14:535–63

Osman A. F. and M. Mariatti. 2006. Properties of Aluminum Filled Polypropylene Composites. *Polymers and Polymer Composites* Vol. 14(6): 623.

Park M. J., J. S. Jeong and J. S. Park. 2012. Flake orientation in injection molding of pigmented thermoplastics. *Journal of Manufacturing Science and Engineering* 134 (1).

Powell, C.E., Beall, G.W. 2006. Physical properties of polymer/clay nanocomposites. *Solid State and Materials Science* 10, 73.

Rawson K. 1999. Controlled orientation of reflective pigment and optical property characterization of injection-molded polypropylene. *Journal of Polymer Engineering and Science* Vol. 39(1): 177-189.

Rojek, M., Stabik, J. 2009. The influence of X-rays on strength properties of polyester vascular system prosthesis. *Journal of Achievements in Materials and Manufacturing Engineering* 35/1: 47.

Santos, I.O., Pontes, A.J., Martins, C.I., Morphological aspects of injection-molded polypropylene with metallic pigments, ANTEC 2013.

Thongruang, W.; Spontak, R. J.; Balik, C. M. 2002. *Polymer* 43: 2279–2286.

Turner Jones A., J. M. Aizlewood and D. R. Beckett. 1964. Makromol Chem Vol 54: 75-134.

Viana, J.C., Billon, N., Cunha, A.M. 2004. The thermomechanical environment and the mechanical properties of injection moldings. Polym. *Eng. Sci.* 44, 1522.

Viana J.C., A.M. Cunha, and N. Billon. 1997. *Polym. Int.* 43, 159.

Wenig W., D. Singh, G. Botzen, and H-G Mosli. 1990. Weld lines in Injection Moulded Polypropylene Parts: Mechanical Properties-Morphology Relationships, Die Angewandre Makmmolekuhre Chemie, 179: 35-56.

Wheeler I. 1999. *Metallic Pigments in Polymers.* UK: Rapra Technology Limited. ISSN 1-85957-166-2.

Williams JG. 2001. A linear elastic fracture mechanics (LEFM) standard for determining KIc and GIc for plastics. In: Moore CR, Pavan A, Williams JG, editors. Fracture mechanics testing methods for polymers, adhesives and composites, vol. ESIS Publication 28. The Netherlands: Elsevier.

Wróbel, G., Kaczmarczyk, J., Stabik, J., Rojek, M. 2009. Numerical models of polymeric composite to simulate fatigue and ageing processes. *Journal of Achievements in Materials and Manufacturing Engineering* 34/1, 31.

Xu W, Liang G, Zhai H, Tang S, Hang G, Pan W-P. 2003. Preparation and crystallization behaviour of PP/PP-g-MAH/Org-MMT nanocomposite. *Eur Polym J* 39:1467–74.

Xu, Y.; Chung, D. D. L. 2001. Mroz, C. *Compos A* 32: 1749–1757.

Yu, S.; Hing, P.; Hu, X. 2002. *Compos A* 33: 289–292.